

Structural and Phase Elemental Distribution in Pulsed Plasma Coating Deposited with Cemented Carbide Cathode

V.G. Efremenko¹, Yu.G. Chabak¹, K. Shimizu², T.V. Pastukhova¹, N. Espallargas³,
V.I. Fedun¹, V.I. Zurnadzhy¹

¹ Priazovskyi State Technical University, 7, Universitetskaia St., 87555 Mariupol, Ukraine

² Muroran Institute of Technology, 27-1, Mizumoto-Cho, 050-8585 Muroran-city, Japan

³ Norwegian University of Science and Technology, 7491 Trondheim, Norway

(Received 20 February 2020; revised manuscript received 15 June 2020; published online 25 June 2020)

The object of this work is to study microstructural features of the coating obtained by pulsed-plasma deposition using cemented carbide WC-TiC-Co as an eroded electrode. The coating was deposited employing an electro-thermal axial plasma accelerator involving a pulse arc discharge with the power reached 20 MW. Cemented carbide (an alloy of T15K6 grade) was used as a tip of the cathode to be eroded under the discharge. The substrate material was low-alloyed structural steel 75Mn1. The investigations included scanning electron microscopy observation (Quanta FEG 650 FEI, Ultra-55 Carl Zeiss), energy-dispersive X-ray spectroscopy (JED-2300, JEOL) and microhardness measurement (FM-300, Future-Tech Corp.) under the load of 20 g. It was shown that after 10 plasma impulses the coating of 95-125 μm thick was obtained tightly adjusted to the modified substrate layer. The coating consisted of high-carbon martensite or martensite/retained austenite matrix with a microhardness of 415-977 HV (mean value of 707 ± 113 HV) and of randomly distributed 2.1 vol. % globular carbides (W,M)C and (Ti,M)C of 0.2-8.5 μm diameter. EDS study revealed that the carbides were alloyed with tungsten and titanium both. It allowed to conclude that carbides were not transferred by plasma flux but they crystallized *in situ* from the melt deposited on the substrate surface. The contribution of cemented carbide to the coating formation was limited by 17 % which was explained by low cemented carbide erosion caused by the high temperature of carbides WC and TiC melting. The coating was mostly composed of the product of the erosion of a steel anode. The matrix was alloyed with the elements (W, Ti, Co, Cu), released from the cathode during its melting/evaporation under the high-current discharge.

Keywords: Pulsed-plasma deposition, Coating, Cemented carbide, Microstructure.

DOI: [10.21272/jnep.12\(3\).03039](https://doi.org/10.21272/jnep.12(3).03039)

PACS numbers: 52.77. - j, 62.20.Qp, 61.66.Dk, 64.70.Kb

1. INTRODUCTION

Among the many approaches undertaken to improve the machine parts and tools durability, the most widely used is a fabrication of a protective coating to enhance the resistance to wear, corrosion, high-temperature oxidation, etc. [1, 2]. Coating formation implies the usage of expendable (eroded) material which could be of different type and shape depending on the technology: a powder (HVOF, LMD), an electrode (arc-welding, PTA), a “target” (PVD), etc. [3, 4]. Pulsed-plasma deposition belongs to cladding technologies providing protective overlay due to plasma-induced transfer of electrode material. High temperature in plasma generator ensures electrodes melting/evaporation with further high-velocity plasma transfer of the materials to be tightly deposited on plasma-heated substrate [5, 6]. The erosion behavior of the material could vary widely depending on its structure-phase status. Thus, the chemical composition and phase constituents of the electrodes are essential to obtain the coating of the required properties [5-7].

The pulsed-plasma modification and deposition applying an electro-thermal axial plasma accelerator (EAPA) are described in previous works [8, 9]. High-current discharge inside EAPA chamber generates short-living plasma formation with high energy density [8]. One of the advantages of EAPA is its adaptability for using eroded electrode of various solid materials. EAPA was applied to get the coating using the axial electrode (cathode) made of mild steel, Al, W, Ti,

bronze, Ni-Cr alloy [9]. Pulsed-plasma coatings with high amount of hard phases (carbides, borides, etc.) are of interest for practical application as-wear-resistant protection. Therefore, the pulsed plasma coatings were obtained by EAPA equipped with the eroded cathode made of wear-resistant alloys highly alloyed by carbide-forming elements (Cr, W, Ti, V), namely HHS steel T1 (18 wt. % W), high-Cr cast iron (28 wt. % Cr), high-boron Cr-Mn-Si-V steel [9]. The mentioned alloys were rather easy-melting due to carbide eutectic in their structure. This caused the intensive erosion of the cathode under arc discharge with liquid material transfer by plasma flux. The micro-droplets solidified on the substrate creating the overlay with “frozen” non-equilibrium structure (oversaturated solid solution) with a “solute-trapping” effect [10]. This implies the consequential post-heat treatment to precipitate the carbides from the matrix which could negatively affect the bulk mechanical properties. In this regard, the carbides should be directly plasma-flux transferred from the cathode to the substrate without melting. Therefore, the further investigation is required to adopt the proper cathode material and the working parameters of electro-thermal axial plasma accelerator. Based on the above, the object of the present work was to investigate the applicability of cemented carbide as eroded electrode of pulsed plasma accelerator. This material is frequently used for thermal spray coating [11]. However, there is no data about its application for plasma-pulsed deposition of the wear-resistant coating.

2. MATERIALS AND METHODS

Pulsed-plasma treatment was performed using EAPA consisting of discharge chamber (an arrester PTF-6-0.5/10U1) and an electrical circuit comprising an energy storage of 1.5 mF capacity. EAPA design and circuit diagram of the electrical connections are outlined more detailed elsewhere [8, 9]. The cathode (a steel rod) was positioned coaxially inside the EAPA chamber. Expendable part of the cathode was a bar with dimensions of 4×5×40 mm made of sintered cemented carbide WC-TiC-Co (grade T15K6) containing 79 vol. % of tungsten carbide (WC), 15 vol. % of titanium carbide (TiC), and 6 vol. % of cobalt binder. The cemented carbide bar was attached to the end of the cathode tip through the cooper mount.

Pulsed-plasma deposition was performed under the following working parameters: the capacity of the energy storage is 1.5 mF; charging voltage is 4.0 kV, the discharge current is up to 18 kA, a number of pulse discharges is 10; inter-electrodes distance inside EAPA chamber is 50 mm; the distance from EAPA edge to the target is 50 mm; an air atmosphere. The substrate was a specimen of 10×10×25 mm in size made of steel grade 75Mn1 (0.75 wt. % C, 0.91 wt. % Mn, 0.28 wt. % Si).

The microstructure of the specimens was examined using the scanning electron microscopes Quanta FEG 650 (FEI) and Ultra-55 (Carl Zeiss). The specimens were prepared according to the standard metallographic procedure using ATM specialized equipment. The polished surface was chemically etched with a 4 vol. % nital reagent. Elemental phase distribution was studied using EDX (JED-2300, JEOL). Microhardness was measured using FM-300 (Future-Tech Corp.) tester at the load of 0.020 kg.

3. RESULTS

3.1 Microstructure Characterization

Fig. 1 illustrates the microstructure of the coating obtained by pulsed-plasma deposition. As seen, the width of the coating varied in the range of 95-125 μm . The coating is smoothly adjusted to the modified layer of 33-40 μm width which appeared on the substrate surface due to the plasma-induced heating/cooling cycle [8]. The microhardness of the modified layer was measured as 520-600 HV. Behind this layer inward, the initial specimen's microstructure (lamellar pearlite) with average microhardness of 235 HV was observed. The coating consisted of a matrix and randomly distributed precipitates. The volume fraction of the precipitates was accounted for 2.1 vol. %. Most of them were globular-shaped to have bright contrast or dark contrast (the latter are shown by the arrows in Fig. 1). The fractions of bright-contrast and dark-contrast precipitates were measured as 1.7 vol. % and 0.4 vol. %, respectively.

Fig. 1 presents the backscattered-electron (BSE) image which allows to roughly identify the phases based on number Z of alloying elements [12]. Bright-contrast globules were enriched with "heavy" elements (presumably W, $Z = 74$). Taking into account the cathode chemical composition they could be considered as WC carbide. Furthermore, dark-contrast precipitates

were enriched by "light" elements (Ti, $Z = 22$) considered as TiC carbide. Accordingly, the matrix was intermediate in contrast assuming its enrichment by iron (Fe, $Z = 26$).

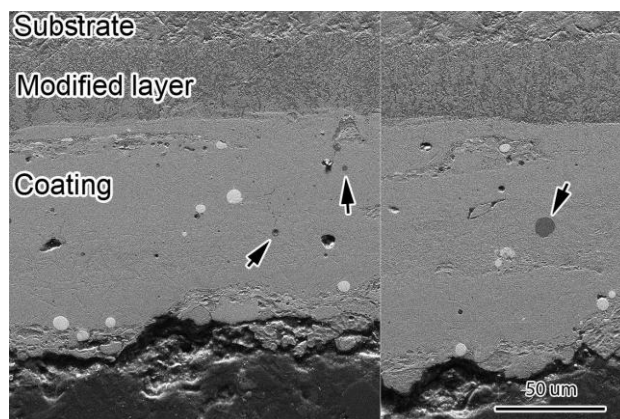


Fig. 1 – BSE image of the coating

The size of the carbides varied in a rather wide range from 0.2 μm to 8.5 μm for WC and from 0.2 μm to 8.0 μm for TiC (Fig. 2). Almost all TiC precipitates were less than 2 μm in size, while WC carbides featured a more widespread distribution of precipitate size. The biggest fraction of WC precipitates (35 %) referred to a 3-4 μm size.

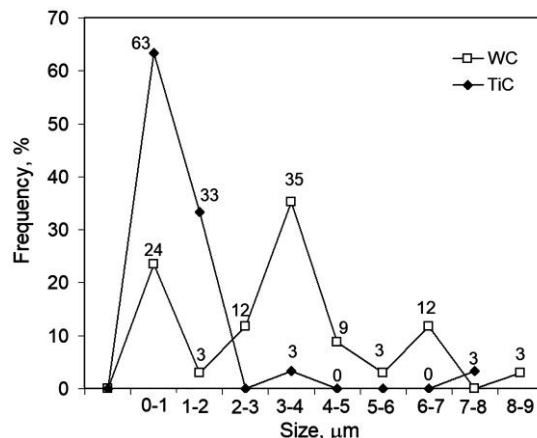


Fig. 2 – The size distribution of the precipitates

The structural peculiarities of the coating are performed in Fig. 3. The main one was WC carbides having a near-spherical shape. The high-magnification observation allowed to reveal a grained pattern of WC precipitate consisting of fine grains of 0.1-1.8 μm diameter. Some of the carbides were fractured as shown in Fig. 3a. The microhardness test was applied for enlarged WC precipitates and their microhardness was measured as 1561-2310 HV with a mean value of 1994 ± 240 HV (which was consistent with the literature data [13]). Apart from globular WC carbides, another morphological type of tungsten carbide was found. It was a thick carbide network that lied around matrix grains creating a eutectic-like area (Fig. 3b, c). "Eutectic" areas were located mostly in the coating outwards layer.

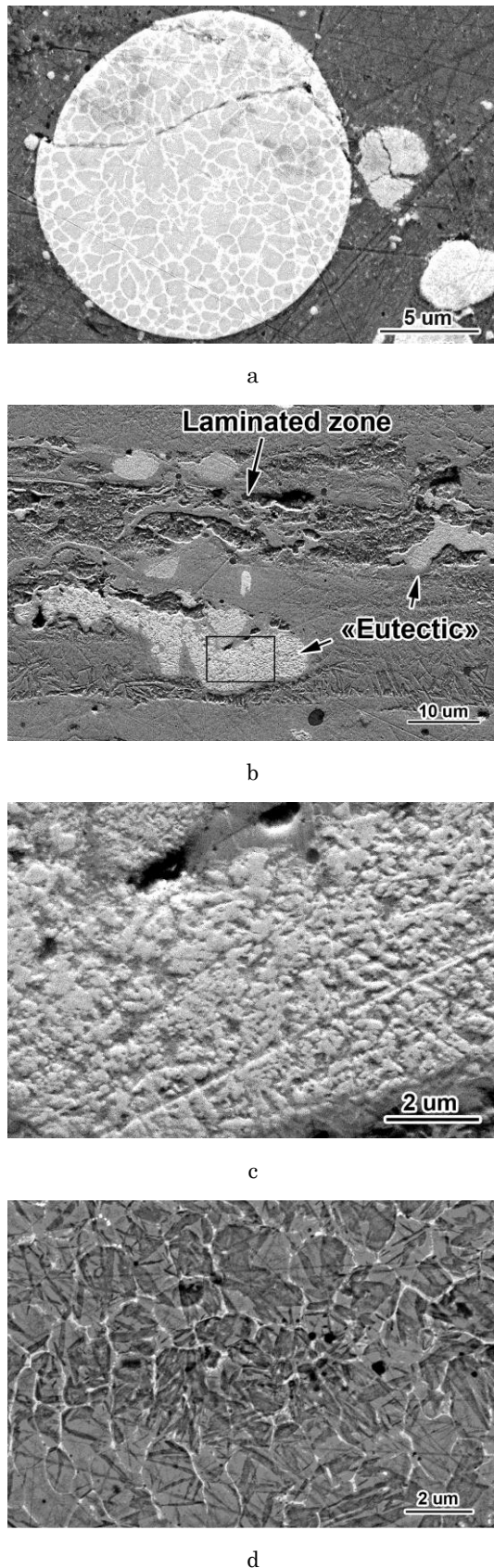


Fig. 3 – Microstructural features of the coating: WC carbide (a), layered morphology and “Eutectic” areas (b), enlarged image of “Eutectics”, denoted in Fig. 3b by the rectangle (c), grain-boundary network with fine martensite needles (d)

The main part of the coating was a matrix having austenite-martensite structure. The presence of martensite was revealed by a needle pattern which is characteristic for high-carbon acicular martensite. The martensitic structure was also proved by high matrix microhardness varying in the range of 412-977 HV with a mean value of 707 ± 113 HV (i.e. 60.5 HRC). Such hardness indicated the carbon content in the matrix to be not less than 0.6 wt. % [14]. The matrix had a laminated texture (Fig. 3b) which reflected the layer-by-layer mechanism of the coating formation.

At half the height of the coating, the matrix featured a grainy pattern with the grains of 0.5-2.0 μm diameter. Thin carbide network was observed lying along the matrix grain boundaries. As seen in Fig. 3d, martensitic needles length was limited by grain size indicating fine-structured martensite morphology.

3.2 Phase Chemical Composition

The phase elemental composition was studied employing the energy-dispersive X-ray spectroscopy. The results of electron probe microanalysis (EPMA) are presented in Table 1. Bright-contrast globular precipitates contained 83 wt. % W and 5.5 wt. % C which was close to the stoichiometry of tungsten carbide WC (93.9 wt. % W and 6.1 wt. % C). The deficiency of tungsten was compensated by titanium (8.9 wt. %) and other elements (Co, Cu, Fe) in a much lesser amount. The presence of W and Ti in globular precipitates was confirmed by the EDX spectra shown in Fig. 4a. Eutectic areas featured slightly decreased levels of W and Ti (as compared with WC globules) in favor of iron. Matrix was found to be Fe-based (80.8 wt. %) while the contents of tungsten and titanium were rather high as for αFe (5.8 wt. % and 0.9 wt. %, respectively) (Fig. 4b). Moreover, in certain matrix areas, the concentration of tungsten was increased even to 17-34 wt. %. Also, 2.6 wt. % Cu was found in the matrix indicating ferrite oversaturation with copper (the solubility limits of Cu in αFe is 0.5 wt. % at 700 $^{\circ}\text{C}$ [15]). The concentration of carbon in the matrix was measured as 8.34 wt. % that was considered as overestimating artefact caused by high EDS sensitivity for carbon contamination [16].

Table 1 – Phase chemical composition (wt. %)

Element	Matrix	Eutectic	WC
C	8.34 ± 5.90	4.23 ± 0.74	5.54 ± 0.39
Mn	0.67 ± 0.08	–	–
Si	0.32 ± 0.05	–	–
W	5.82 ± 0.52	78.67 ± 10.35	83.02 ± 2.1
Ti	0.95 ± 0.13	7.66 ± 0.95	8.85 ± 1.60
Co	0.53 ± 0.21	0.16 ± 0.03	1.10 ± 0.56
Cu	2.60 ± 0.39	0.37 ± 0.15	0.60 ± 0.24
Fe	80.77 ± 9.25	16.58 ± 11.45	0.83 ± 0.17

The distribution of some elements within the coating was visualized using EDS-mapping presented in Fig. 5. On mapping, the quantity of the element is shown by the color according to a left-side color bar. As seen in Fig. 5b, tungsten is mostly concentrated in globular precipitates throughout the coating. Tungsten was segregated in the inner layer of the coating adjust-

ed to the substrate where its concentration was EPMA-measured as 5.8 wt. %. In contrast, the outer layer was depleted by tungsten with its content of about 0.9 wt. %. Titanium distribution (Fig. 5c) was almost the same as that of tungsten. This clearly proves that globular precipitates contained W and Ti both. Moreover, Fig. 5a-c illustrate a roundish precipitate circled by the dotted line. As seen, this precipitate gives higher contrast response for titanium (Fig. 5c) than that for tungsten (Fig. 5b) indicating that the precipitate was Ti-rich carbide with minor addition of tungsten. This observation supports the above BSE-based assumption that globular dark-contrast precipitates were TiC carbides. Fig. 5d shows that all carbides were almost free of iron while iron content in the coating was decreased as compared with the substrate.

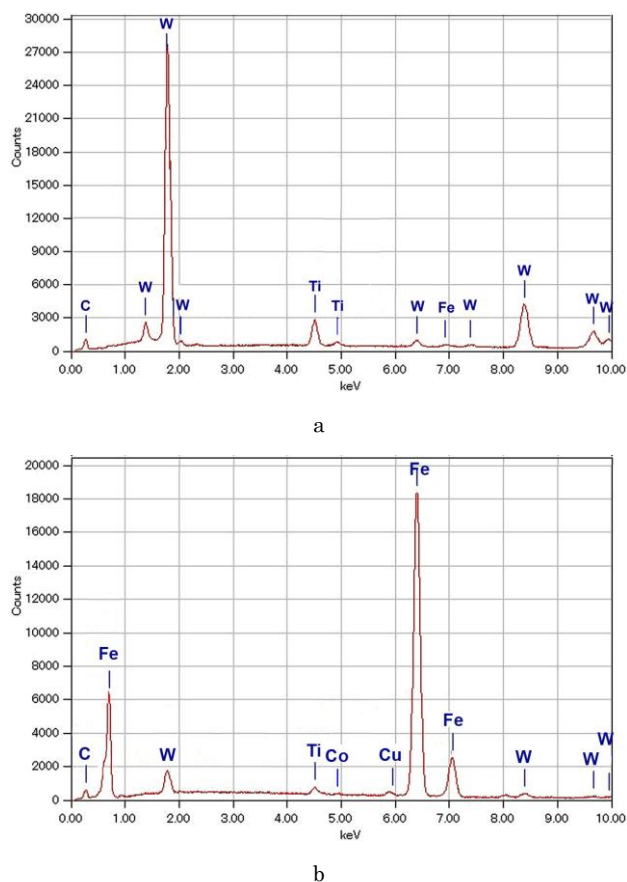
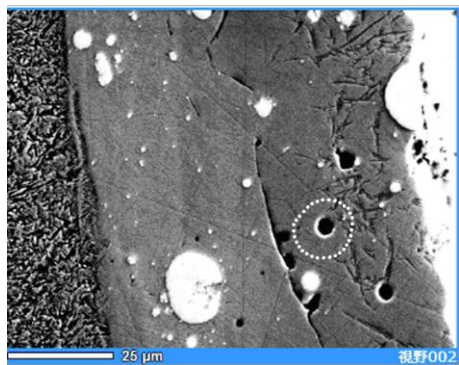
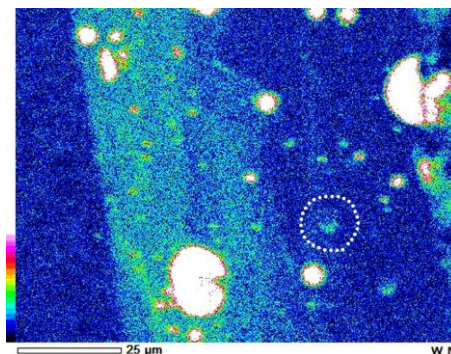


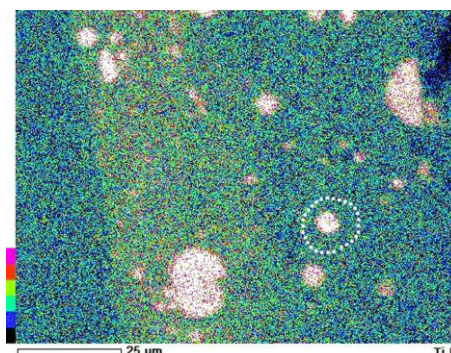
Fig. 4 – EDX spectra from carbide WC (a), from the matrix (b)



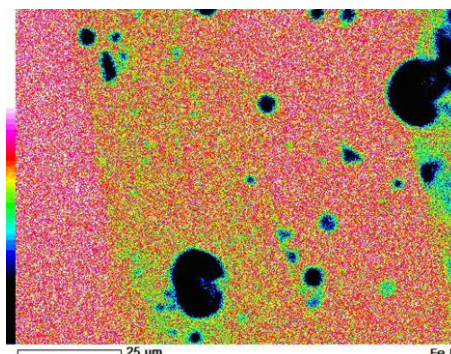
a



b



c



d

Fig. 5 – SEI image of the coating (a) and corresponding EDS-mapping of W (b), Ti (c) and Fe (d) distributions

4. DISCUSSION

The presented results showed that pulsed-plasma deposition using cemented carbide cathode resulted in the coating consisting mostly of a martensite matrix with a low amount of carbide precipitates. The most interesting was the shape and chemical composition of the precipitates. The angular precipitates which are characteristic for cemented carbide were not observed in the coating; instead, all carbides had a nearly spherical shape. This meant that the carbides were either partially melted (edge-rounded) being transferred by the plasma flux or they solidified directly from the melt. The latter assumption was supported by the fact that all carbides were simultaneously alloyed by W, Ti, and Co while cemented carbide was sintered from technically pure WC and TiC without impurities. These features allow to conclude that carbide precipitates

were not transported by plasma flux in the initial state, on the contrary, they crystallized in situ during the coating solidification. Accordingly, the precipitates absorbed different elements dissolved in the melt.

Presumably, initial WC and TiC carbides evaporated/melted from the cathode (cemented carbide) surface under the arc discharge. The atoms/ions of W, Ti, C, and Co joined the plasma gas or they were in the micro-droplets to be transferred by plasma flux to the substrate. When the micro-droplets reached the substrate they were additionally W(Ti)-implanted from plasma gas. Then carbides WC and TiC crystallized in a liquid to be nucleated on the fluctuations of tungsten or titanium atoms respectively. Considering ultra-high cooling rate after plasma heating (estimated as about $5.5 \cdot 10^6$ K/s [8]) carbide formation presumably proceeded by non-equilibrium path involving the atoms of other elements present in the melt in fluctuation vicinity. Therefore, W-based and Ti-based carbides were alloyed by other elements found in the coating (Ti, W, Co, Cu, Fe). Based on chemical composition (Table 1) the stoichiometry of WC carbide in the coating can be presented as $(W_{0.964}Ti_{0.027}Fe_{0.003}Co_{0.004}Cu_{0.002})C_{0.90}$.

Once crystallized the carbide particles were subjected to the stress caused by the matrix thermal contraction under the cooling. The magnitude of the stress is proportional to the difference between the coefficient of thermal expansion of the carbide ($4.5 \cdot 10^{-6} K^{-1}$) and the austenitic matrix ($16 \cdot 10^{-6} K^{-1}$) [17]. In case of cooling from solidus temperature (1400 °C for steel with 0.6 wt. % C) to room temperature, thermal stresses could be of 4.53 GPa (for steel modulus $E = 200$ GPa). This value roughly corresponds to the tensile compression strength of tungsten carbide (4-8 GPa [13]), so such stresses might lead to the rupture of carbides [18], especially of large carbide particle.

The formation of tungsten carbides proceeded also through a eutectic reaction in the liquid areas with a decreased concentration of tungsten leading to the appearance of eutectic structure (Fig. 3b, c). Tungsten and titanium were also dissolved in the matrix in much less content. Considering the phase volume fractions and phase chemical compositions the mean concentration on tungsten in the coating was estimated as about 17 wt. %. This fact indicates the low degree of cemented carbide participation in the deposition process. The rest of the coating fraction consisted mostly of iron, while this element was not included in cemented carbide composition. And if so, then steel flange (acting as EAPA anode) was the main source of the coating material. Besides, copper also took part in the coating formation being the constituent of the cathode. However, copper contribution to the coating was minor due to the large difference in the electrical resistance of the plasma and cemented carbide. According to the results of [8], the specific resistance of the plasma exceeds 200 $\mu\Omega \cdot m$, which is several orders of magnitude higher than that of cemented carbide (0.19 $\mu\Omega \cdot m$ [19]), while their cross-sectional areas were comparable. Therefore, the displacement of the discharge "spots" from the cathode tip to the copper mount was highly unlikely.

The main reason for low cathode erosion refers to the thermo-physical properties of the cemented carbide

components. Melting points of WC and TiC are rather high (2785 °C and 3160 °C, respectively [17]) that prevented an intensive erosion of the cathode surface. On the other hand, the negligible volume fraction of a binder (Co) did not provide an easy release of the carbides through the binder melting [20]. Moreover, the carbides particles were diffusively bound to each other under high-temperature sintering making its release even more difficult. Therefore, cemented carbide moderately contributed to the coating formation.

The high microhardness of the matrix indicated the microstructure of martensite that was also proven by the needle morphology. Such morphology is specific for high-carbon martensite while the steel elements of the electrodes were made of mild (low-carbon) steel. High-carbon steel was formed due to the plasma-enrichment of melt by carbon atoms released from cemented carbide and due to evaporation of inner dielectric walls of the EAPA chamber [9]. It can be assumed that carbon was unevenly distributed in the coating which might result in retained austenite along with martensite. The wide range of matrix microhardness values (412-977 HV) might be due to different martensite/retained austenite ratio. The distinctive feature of the matrix was its fine-crystalline structure. The grain boundaries were clearly revealed due to the thin carbide network engulfing the grains. This network formation was obviously caused by matrix enrichment with carbon and carbide-forming elements (W, Ti) and it was promoted by the repetitive heating under the plasma flux.

The results obtained revealed the possibility of fabricating a pulsed plasma coating with WC/TiC carbides without additional post-plasma heat treatment. However, the analysis of the coating microstructure showed that the volume fraction of carbide precipitates is not appropriate to ensure high wear resistance of the coating. Further design of the cathode is required to intensify its erosion while the carbides should be plasma-transferred in the non-melted state. A composite material comprising hard-to-melt carbides and easy-to-melt binder can be a prospective candidate for EAPA cathode with the corresponding adjustment of EAPA working parameters.

5. CONCLUSIONS

The use of an electro-thermal axial plasma accelerator with cemented carbide cathode (an alloy of T15K6 grade), allowed to obtain after 10 plasma impulses the coating of 95-125 μm thick with a microhardness of 415-977 HV. The coating had high-carbon martensite or martensite-austenite structure with 2.1 vol. % of randomly distributed globular precipitates of (W,M)C and (Ti,M)C carbide of 0.2-8.5 μm diameter. The microhardness of WC carbides was measured as about 2000 HV. The formation of the martensite-carbide coating structure occurred directly during pulse-plasma treatment without post-plasma heat treatment. It was proved that carbides contained tungsten and titanium both indicating its crystallization from the melt deposited on the substrate surface. Some parts of W-rich carbide solidified as a eutectic. Carbides and a matrix were also alloyed by Fe, W, Ti, Co, and Cu, released through the electrodes melting/evaporation under the

high-current discharge. The contribution of cemented carbide to the coating was 17 wt. % while the most fraction of the coating was formed due to erosion of a steel anode. Such behavior was presumably caused by the high temperature of carbides WC and TiC melting.

REFERENCES

1. V. Pidkova, I. Brodnikovska, Z. Duriagina, V. Petrovskyy, *Funct. Mater.* **22** No 1, 34 (2015).
2. M.A. Vasylyev, B.N. Mordyuk, S.I. Sidorenko, S.M. Voloshko, A.P. Burmak, I.O. Kruhlov, V.I. Zakiev, *Surf. Coat. Technol.* **361**, 413 (2019).
3. A.D. Pogrebnyak, S.N. Bratushka, M.V. Il'yashenko, N.A. Makhmudov, O.V. Kolisnichenko, Yu.N. Tyurin, V.V. Uglov, A.V. Pshik, M.V. Kaverin, *J. Friction Wear* **32** No 2, 84 (2011).
4. O.V. Sobol, A.A. Andreev, A.A. Meylekhov, A.A. Postelnyk, V.A. Stolbovoy, I.M. Ryshchenko, Yu.Ye. Sagaidashnikov, Zh.V. Kraievskaya, *J. Nano-Electron. Phys.* **11** No 1, 01003 (2019).
5. M. Kovaleva, Y. Tyurin, N. Vasilik, O. Kolisnichenko, *Surf. Coat. Technol.* **232**, 719 (2013).
6. O.V. Sobol, A.A. Andreev, R.P. Mygushchenko, V.M. Beresnev, et al. *Probl. At. Sci. Technol., Ser.: Plasma Phys.* **113**, No 1 82 (2018).
7. Y.Y. Özbek, H. Akbulut, M. Durman, *Vacuum* **122**, 90 (2015).
8. Yu.G. Chabak, V.I. Fedun, T.V. Pastukhova, V.I. Zurnadzhy, S.P. Bereznyy, V.G. Efremenko, *Probl. At. Sci. Technol., Ser.: Plasma Phys.* **110** No 4, 97 (2017).
9. Yu.G. Chabak, V.I. Fedun, V.G. Efremenko, T.V. Pastukhova, B.V. Efremenko, *Probl. At. Sci. Technol., Ser.: Plasma Phys.* **123** No 5, 167 (2019).
10. T. Zheng, B. Zhou, Y. Zhong, J. Wang, S. Shuai, Z. Ren, F. Debray, E. Beaugnon, *Sci. Rep.* **9**, 266 (2019).
11. L.-M. Berger, *Int. J. Refract. Met. Hard Mater.* **49**, No 1, 350 (2015).
12. T. Kowoll, E. Müller, S. Fritsch-Decker, S. Hettler, H. Störmer, C. Weiss, D. Gerthsen, *Scanning article ID 4907457* (2017).
13. A.S. Kurlov, A.I. Gusev, *Tungsten carbides: Structure, properties and application in hardmetal* (Springer Science & Business Media: 2013).
14. V.G. Efremenko, O. Hesse, Th. Friedrich, M. Kunert, M.N. Brykov, K. Shimizu, V.I. Zurnadzhy, P. Suchmann, *Wear* **418-419**, 24 (2019).
15. O.K. von Goldbeck, *Iron-Copper. In: Iron-Binary Phase Diagrams* (Berlin: Springer: 1982).
16. M. Scimeca, S. Bischetti, H.K. Lamsira, R. Bonfiglio, E. Bonanno, *Eur. J. Histochem.* **62** No 1, 2841 (2018).
17. *Ceramics Science and Technology. Volume 4: Applications.* (Ed. R.Riedel, I-Wei Chen) (Wiley-VCH Verlag GmbH Co. KGaA: 2013).
18. A. Anishchenko, V. Kukhar, V. Artiukh, O. Arkhipova, *MATEC Web of Conferences.* **239**, 06006 (2018).
19. H.O. Pierson, *Handbook of refractory carbides & nitrides: Properties, characteristics, processing and applications*, (Noyes Publications: 1996).
20. O. Sukhova, Yu. Syrovatko, *Metallofiz. Noveishie Tekhnol.* **33**, 371 (2011).

Структурний і фазово-елементний розподіл у імпульсному плазмовому покритті, отриманому з використанням твердосплавного катоду

В.Г. Єфременко¹, Ю.Г. Чабак¹, К. Шимізу², Т.В. Пастухова¹, Н. Еспалларгас³,
В.І. Федун¹, В.І. Зурнаджі¹

¹ Приазовський державний технічний університет, вул. Університетська, 7, 87555 Маріуполь, Україна

² Muroran Institute of Technology, 27-1, Mizumoto-Cho, 050-8585 Muroran-city, Japan

³ Norwegian University of Science and Technology, 7491 Trondheim, Norway

Метою даної роботи є дослідження мікроструктурних особливостей покриття, одержаного імпульсно-плазмовою обробкою з використанням твердого сплаву WC-TiC-Co (T15K6) у якості розхідного (еродуючого) електрода. Покриття наносили на низьколеговану конструкційну сталь 75Г1 за допомогою електротермічного аксіального плазмового прискорювача з потужністю дугового розряду до 20 МВт. В роботі використали мікроскопічний аналіз (за допомогою скандувальних мікроскопів Quanta FEG 650 FEI та Ultra-55 Carl Zeiss), енергодисперсійну спектроскопію (JED-2300, JEOL) та вимірювання мікротвердості (FM-300, Future-Tech Corp.) при навантаженні 20 г. Було встановлено, що після 10 плазмових імпульсів на поверхні сталі утворилось покриття товщиною 95-125 нм, а між покриттям та основою виник модифікований сталевий шар товщиною 33-40 мкм. Покриття складалось із матриці зі структурою високовуглецевого мартенситу або суміші мартенситу і залишкового аустеніту з мікротвердістю 415-977 HV (середнє значення 707 ± 113 HV). В межах матриці виявлено випадково розташовані глобулярні карбіди, збагачені вольфрамом (W,M)C або титаном (Ti,M)C діаметром 0,1-9,1 мкм. Загальна об'ємна частка карбідів становила 15 %. EDS дослідження показало, що карбіди одночасно вміщували як вольфрам, так і титан, тобто вони не були «відірвані» з катоду і перенесені плазмовим потоком, а утворились *in situ* із рідини при кристалізації покриття. Матеріальний вклад катоду в формування покриття не перевищив 17 %, що пояснюється незначною ерозією твердого сплаву через високу температуру плавлення карбідів WC і TiC. Покриття в основному складалось з продуктів ерозії сталевого електрода (аноду) плазмового прискорювача. Матриця покриття виявилась легованою рядом елементів (W, Ti, Co, Cu), які еродували з поверхні катоду під час його плавлення та випаровування під дією високострумного розряду в камері прискорювача.

Ключові слова: Імпульсно-плазмове нанесення, Покриття, Твердий сплав, Мікроструктура.